Current Applied Physics 11 (2011) 1188–1191

Contents lists available at ScienceDirect

Current Applied Physics

journal homepage: www.elsevier.com/locate/cap

Strong coupling optimization with planar spiral resonators

Avraham Klein, Nadav Katz*

Racah Institute of Physics, Hebrew University of Jerusalem, Edmond J. Safra Campus, Givat Ram, Israel

ARTICLE INFO

Article history:
Received 24 December 2010
Received in revised form
21 February 2011
Accepted 21 February 2011
Available online 1 March 2011

Keywords:
Wireless power transfer
Resonant coupling
Electromagnetic devices

ABSTRACT

Planar spirals offer a highly scalable geometry appropriate for wireless power transfer via strongly coupled inductive resonators. We numerically derive a set of geometric scale and material independent coupling terms, and analyze a simple model to identify design considerations for a variety of different materials. We use our model to fabricate integrated planar resonators of handheld sizes, and optimize them to achieve high-Q factors, comparable to much larger systems, and strong coupling over significant distances with approximately constant efficiency.

1. Introduction

Wireless power transfer via resonant magnetic coupling has attracted considerable attention in recent years. This is due both to its elegance and to its possible applicability at many different size scales, from powering spaceships and cars [1,2], and down to handheld scale devices [3] and microdevice coupling [4]. Such coupling depends strongly on two predominantly geometric properties: The devices involved must be high quality resonators, and they must have far-reaching magnetic fields [5,6]. Thus, the geometric design of the resonators is of utmost importance. Moreover, the geometry of a device is inherently size independent, and this means that if a design exists that can be built at different size scales, using different materials, then the same considerations will apply to all variations. The planar spiral is such a design, being both simple and quasi two-dimensional. Thus, for example, planar spiral designs can easily be etched on a thin substrate and incorporated into current handheld devices.

In this Letter, we analyze a planar spiral model and numerically computed coupling terms in order to identify optimal design considerations for different materials at a desired size scale. For example, we show how high T_C superconductors can be designed so as to achieve very strong coupling. We use our method to optimize the design of a device similar in size to currently used handheld devices, using inexpensive materials, by identifying the properties of the dominant dielectric loss channel for the size/materials involved and using capacitative loading to compensate. We achieve very high-Q factors that are typical of much larger devices and strong coupling over significant ranges. We then show that the coupling between the devices is robust, being almost constant over the entire coupling range.

2. Theoretical model

Coupling between two high-Q resonators is adequately described by Coupled-Mode Theory [5,7]. A source and destination device can be represented by complex-valued variables a_1, a_2 normalized so that $|a_n^2|$ is the energy in a resonator, obeying the relation:

$$-i\omega a_1 = -[i\omega_0 + \Gamma_1]a_1 + i\kappa a_2 + F \tag{1}$$

$$-i\omega a_2 = -[i\omega_0 + \Gamma_2]a_2 + i\kappa a_1 \tag{2}$$

where $\Gamma_m = (1 + k_m)\gamma_m$ is the loaded dissipation factor of the device, k_m is a coupling coefficient to some load or measuring device and $\gamma_m = \frac{\omega_0}{2Q_m}$ is the unloaded dissipation factor. κ represents the coupling between the two devices and F is a forcing term for the source a_1. Solving Eq. (1)–(2) yields frequency splitting: $|a_2|^2$is maximized and the devices transfer energy efficiently when $\omega - \omega_0 = \pm\sqrt{\kappa^2 - (\Gamma_1^2 + \Gamma_2^2)/2}$. The regime where this splitting takes place is called the strong coupling regime. For identical resonators ($k_1 = k_2 = k_c, \gamma_1 = \gamma_2 = \gamma$) this splitting is possible when:

* Corresponding author. Tel.: +972 2 6586745; fax: +972 2 6586347.
E-mail addresses: avraham.klein@mail.huji.ac.il (A. Klein), katzn@phys.huji.ac.il (N. Katz).

1567-1739/$ – see front matter © 2011 Elsevier B.V. All rights reserved.
doi:10.1016/j.cap.2011.02.017

$$\frac{\kappa}{(1+k_c)\gamma} \geq 1 \tag{3}$$

Thus a Figure of Merit for such a system is the quantity $\kappa/\gamma = Qk$ where k is a dimensionless coupling term. In this we assume $k_c \leq 1$ so as to maintain the strong coupling, or equivalently, keep the loaded quality factor of the devices high. For magnetically coupled systems $k = M/L$, M, L, being the mutual and self inductances of the devices respectively. The efficiency in this regime for identical resonators at the split frequencies is constant and obeys:

$$\eta = \frac{k_c}{2(1+k_c)} \tag{4}$$

The upper limit of $\eta \leq 1/4$ (for $k_c \leq 1$) appears because the devices are identical. Higher efficiency is obtained with proper loading [7,6].

Such coupling can be achieved by using planar spiral resonators driven at quasi-static frequencies. It is well known that such resonators can be modeled as lumped RLC resonant circuits. For a description of the considerations involved in modeling spirals and related planar spirals, we refer the reader to Refs. [8,9]. Fig. 1 shows the schematic of such a setup and a simple equivalent circuit for a spiral. Such a resonator is described by inner and outer diameters d_i, d_o, number of loops n and loop width w, and has a resonant frequency ω_0. Additionally, an underpass strip usually connects the spiral inner and outer extremities, at a separation d_u. Fig. 2 shows a sketch of a basic spiral. Effective L values can be found using current sheet approximations [10]. The capacitance can be written as $C = C_l + C_p$, where C_l, C_p are the inter-coil and coil-underpass capacitances, approximated with coplanar waveguide [11,12](with loops coupling in series) and parallel-plate [13] formulas. The coupling coefficient $k = M/L$ can be extracted numerically. In this work we constructed a table of $k(n, w, d)$ values (d being the coplanar distance between spirals) using the Fasthenry multipole expansion tool [14](see Fig. 3a). These values are scale/material independent so that the same table predicts behavior and design parameters for a wide variety of possible designs. Finally the metallic losses consist of radiative and ohmic losses:

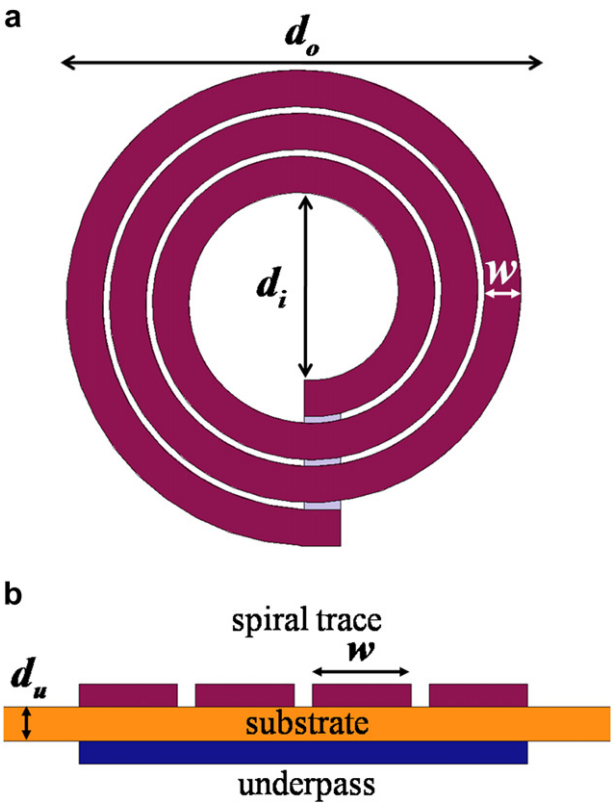

Fig. 2. Sketch of a basic spiral design, and the spiral parameters referred to in our theoretical model. (a) Top-down view, with substrate layer hidden. (b) Side view, with substrate layer.

$$R = \frac{1}{\sigma\xi} \times \frac{2\pi \sum r_i}{2w \cdot \delta_s} + \sqrt{\frac{\mu_0}{\epsilon_0}} \left[\frac{\pi}{6} \left(\frac{\omega}{c}\right)^4 \left(\sum_{i=1}^{n} r_i^2 \right)^2 + \frac{4n^2}{3\pi^3} \left(\frac{\omega}{c}\right)^2 d_u^2 \right] \tag{5}$$

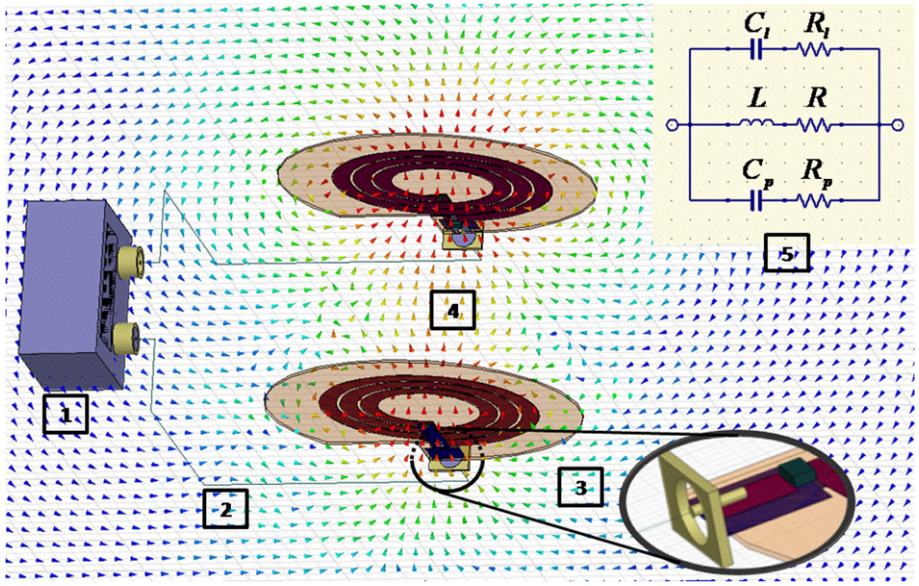

Fig. 1. Schematic of the experimental setup. A network analyzer (1) is connected via coaxial feedlines (2) to a pair of coplanar coupled spirals (the spiral geometry is detailed in Fig. 2). Each spiral is matched to the feedlines via a bonded chip capacitor (3). The S-parameters can be analyzed to obtain the Q factor, coupling and power transfer efficiency between devices. The figure also shows a numerical simulation of the magnetic coupling fields (4), computed using HFSS 11. (5) shows a simplified lumped-element circuit that we have used in our theoretical model.

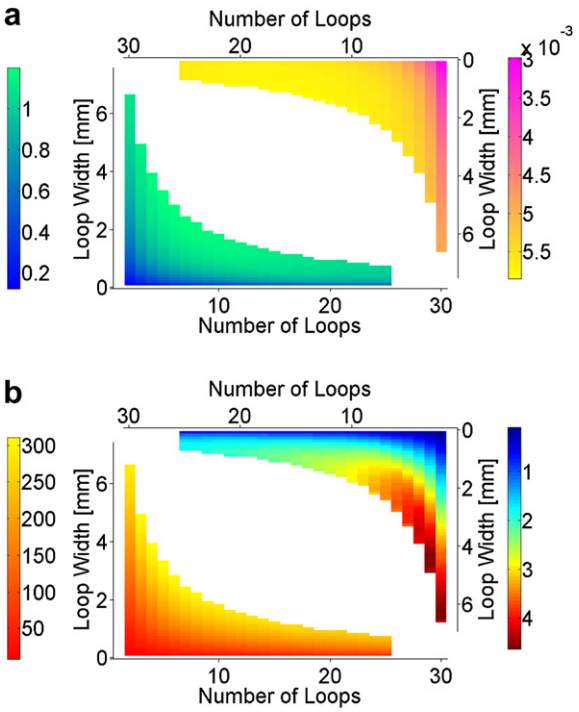

Fig. 3. QM/L optimization for various designs, showing that reducing dielectric and ohmic losses changes design considerations and quality. The model dimensions used are the same as that of Device #1 detailed later. (a) Upper right: The coupling coefficient table k (n, w, $d = 1.8d_o$) used in the analysis in this work. *Lower left*: QM/L for a copper spiral on a Rogers 4350B substrate. Ohmic and dielectric losses dominate. (b) Upper right: QM/L for a copper spiral on a sapphire substrate. Ohmic losses dominate, and removing the dielectric loss allows a very clear preferred design. Lower left: QM/L for a superconducting YBCO film on sapphire (assumed conductivity: $5 \times 10^3 \sigma_{Cu}$ [16]). Metallic losses dominate but the ohmic loss reduction yields two orders of magnitude better performance.

where the first term represents ohmic losses: σ, δ_s are the trace conductivity and skin depth, ξ is an empirical current-crowding factor [15], and $\sum r_i$ is an approximation to the spiral length as a sum of concentric circles with respective radii r_i The second term describes magnetic and electric dipole resistance. The resistances of the capacitative channels R_p, R_l are determined by the substrate loss tangent $\tan\delta$. The quality factor of the spiral is then:

$$Q = \left(\tan\delta + \frac{R}{\omega_0 L}\right)^{-1} \tag{6}$$

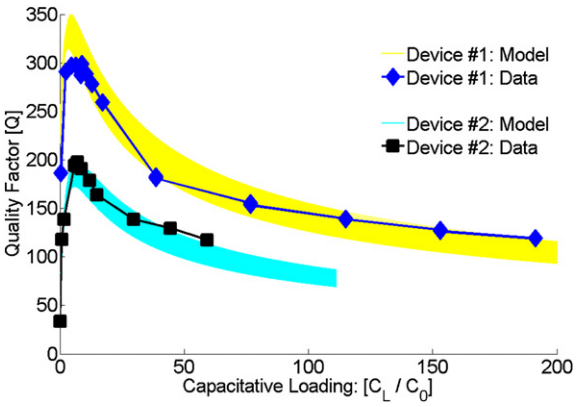

Fig. 4. Capacitative optimization of individual resonators. Note the sharp peak at $C_L/C_0 \sim 7$.

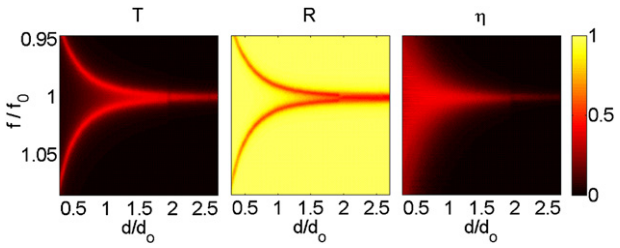

Fig. 5. Coupling and efficiency vs. distance. In the strong coupling regime efficiency is high and frequency independent, but transmission is significant only at the split frequencies.

Examining Eq. (6) leads to a number of conclusions. First, the only scale-dependent factor influencing QM/L is the ohmic loss channel in R. In all other terms (radiation loss, inductance and capacitance) the scale dependencies cancel out. Next, $\tan\delta$is independent of both scale and geometry. Therefore when dielectric loss dominates one cannot optimize the design. However, adding a high quality capacitance C_{ext} in parallel will both reduce the effective loss, i.e. $\tan\delta \to \tan\delta \frac{C}{C + C_{ext}}$, and allow optimization reducing other losses to be significant. Specifically, reduction of loop number and wide traces are crucial, as they lead to a reduction of the term $\sum r_i/w$. Finally, if the ohmic losses can be reduced to the order of radiative losses, for example by using superconductors, then a single optimal design can be adapted to many different scales. Fig. 3 shows actual design scans confirming these conclusions.

3. Experimental results and discussion

Two devices were built to test the coupling efficiency and design optimization. Device dimensions were $d_o = 60$ mm, $n = 3$ mm, $w = 4.4$ mm. and $d_i/d_o = 0.33$ (considered optimal [4]). Device #1 was fabricated on a 0.51 mm thick Rogers 4350B substrate ($\tan\delta = 0.0037$). Device #2 was fabricated on 1.55 mm thick FR4 ($\tan\delta \simeq 0.0180$). The devices were matched to an Agilent N5230A network analyzer as in Fig. 1. High-Q RF chip capacitors ($Q > 1000$) were soldered in series for network matching and in parallel for design optimization.

Fig. 4 shows the Q factor of devices as a function of loading, showing that for optimal loading a sharp peak is obtained, as predicted by Eq. (6), with added capacitance affecting the $\tan\delta, \omega_0, R$ terms. $Q \simeq 300$ for Device #1 at the maximum, which is comparable

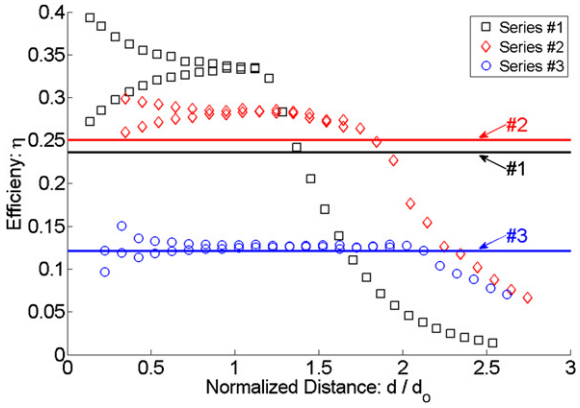

Fig. 6. Efficiency and range of coupling. The measured efficiency is taken as $\eta = \frac{T^2}{1 - R^2}$. The horizontal lines (labeled by series) are those predicted by Eq. (4) when naively assuming identical devices: $Q = 0.5(Q_1 + Q_2), k = 0.5(k_1 + k_2)$.

Table 1
Coupled devices. $[Q_m^L = \frac{\omega_0}{2\Gamma_m}]$.

Series	Device	Q_1, Q_2	k_1, k_2	Q_1^L, Q_2^L
1	2	139,141	0.79,0.99	77,71
2	1	261,281	1.11,0.89	123,149
3	1	274,261	0.34,0.30	205,201

to Q factors of air cored designs an order of magnitude larger [3,7,17]. The theoretical area shown is for $3.5 \leq \xi \leq 4.6$, so using $\xi = 4$ should give accurate results, and this is the number used in all theoretical simulations in this work.

Figs. 5 and 6 detail three coupling experiments whose parameters are given in Table 1.

Fig. 5 shows a sample of the frequency splitting as a function of distance, demonstrating that only at the split frequency is power transfer both efficient and appreciable. Fig. 6 compares the predicted and measured efficiency for the three measurements. For series #2, #3 Eq. (4) gives a good prediction, with the slight disagreement explained by the assumption of identical resonators. For series #1 however the efficiency considerably outstrips the estimate. This is probably because with low Q a first order approximation no longer properly predicts the coupling between resonators. For series #2, #3 strong coupling is achieved for distances of the order $\sim 2d_o$.

To summarize, we have shown how a simple model of spiral inductor resonators can be used to design coupled systems for many different materials and size scales, by identifying crucial geometric considerations. We have shown that proper capacitative coupling using high-Q capacitors and increased trace width can greatly improve quality. We fabricated integrated devices of a similar size to current handheld devices and achieved very high-Q factors and strong coupling over large distances.

Acknowledgement

We acknowledge the support of ISF grant no. 1248/10.

References

[1] R.J. Sedwick, Long range inductive power transfer with superconducting oscillators, Annals of Physics 325 (2) (2010) 287–299.
[2] T. Imura, H. Okabe, Y. Hori, Basic experimental study on helical antennas of wireless power transfer for electric vehicles by using magnetic resonant couplings, in: Vehicle Power and Propulsion Conference, 2009. VPPC '09. IEEE, 2009, pp. 936–940.
[3] F. Segura-Quijano, J. García-Cantón, J. Sacristán, T. Osés, A. Baldi, Wireless powering of single-chip systems with integrated coil and external wire-loop resonator, Applied Physics Letters 92 (2008).
[4] M. Ghovanloo, S. Atluri, A wide-band power-efficient inductive wireless link for implantable microelectronic devices using multiple carriers, Circuits and Systems I: Regular Papers, IEEE Transactions on 54 (10) (2007) 2211–2221.
[5] H.A. Haus, Waves and Fields in Optoelectronics. Prentice-Hall, Inc., 1984, ch. 7.
[6] A. Karalis, J. Joannopoulos, M. Soljacic, Efficient wireless non-radiative mid-range energy transfer, Annals of Physics 323 (1) (2008) 34–48.
[7] A. Kurs, A. Karalis, R. Moffatt, J.D. Joannopoulos, P. Fisher, M. Soljacic, Wireless power transfer via strongly coupled magnetic resonances, Science 317 (5834) (2007) 83–86.
[8] F. Bilotti, A. Toscano, L. Vegni, Design of spiral and multiple split-ring resonators for the realization of miniaturized metamaterial samples, Antennas and Propagation, IEEE Transactions on 55 (8) (2007) 2258–2267. doi:10.1109/TAP.2007.901950.
[9] F. Bilotti, A. Toscano, L. Vegni, K. Aydin, K. Alici, E. Ozbay, Equivalent-circuit models for the design of metamaterials based on artificial magnetic inclusions, Microwave Theory and Techniques, IEEE Transactions on 55 (12) (2007) 2865–2873. doi:10.1109/TMTT.2007.909611.
[10] S. Mohan, M. del Mar Hershenson, S. Boyd, T. Lee, Simple accurate expressions for planar spiral inductances, Solid-State Circuits, IEEE Journal 34 (10) (1999) 1419–1424.
[11] K.C. Gupta, R. Garg, I. Bahl, P. Bhartia, Microstrip Lines and Slotlines, Artech House (1996).
[12] P. Pieters, K. Vaesen, S. Brebels, S. Mahmoud, W. De Raedt, E. Beyne, R. Mertens, Accurate modeling of high-q spiral inductors in thin-film multilayer technology for wireless telecommunication applications, Microwave Theory and Techniques, IEEE Transactions on 49 (4) (2001) 589–599.
[13] W. Gao, Z. Yu, Scalable compact circuit model and synthesis for rf cmos spiral inductors, Microwave Theory and Techniques, IEEE Transactions on 54 (3) (2006) 1055–1064.
[14] M. Kamon, M. Tsuk, J. White, Fasthenry: a multipole-accelerated 3-d inductance extraction program, Microwave Theory and Techniques, IEEE Transactions on 42 (9) (1994) 1750–1758.
[15] T.L. Peck, R.L. Magin, P.C. Lauterbur, Design and analysis of microcoils for nmr microscopy, Journal of Magnetic Resonance, Series B 108 (2) (1995) 114–124.
[16] M. Lancaster, Passive Microwave Device Applications of High-Temperature Superconductors. Cambridge University Press, 2006.
[17] A.P. Sample, D.A. Meyer, J.R. Smith, Analysis, Experimental Results, and Range Adaptation of Magnetically Coupled Resonators for Wireless Power Transfer, Industrial Electronics, IEEE Transactions on 58 (2) (2011) 544–554. doi:10.1109/TIE.2010.2046002.